

1-1-1974

# Application of Monte Carlo criticality calculations to the Ames Laboratory Research Reactor

Donald L. Hull  
*Iowa State University*

Follow this and additional works at: <https://lib.dr.iastate.edu/rtd>

 Part of the [Engineering Commons](#)

## Recommended Citation

Hull, Donald L., "Application of Monte Carlo criticality calculations to the Ames Laboratory Research Reactor" (1974). *Retrospective Theses and Dissertations*. 18327.  
<https://lib.dr.iastate.edu/rtd/18327>

This Thesis is brought to you for free and open access by the Iowa State University Capstones, Theses and Dissertations at Iowa State University Digital Repository. It has been accepted for inclusion in Retrospective Theses and Dissertations by an authorized administrator of Iowa State University Digital Repository. For more information, please contact [digirep@iastate.edu](mailto:digirep@iastate.edu).

Application of  
Monte Carlo criticality calculations  
to the Ames Laboratory Research Reactor

by

Donald L. Hull

A Thesis Submitted to the  
Graduate Faculty in Partial Fulfillment of  
The Requirements for the Degree of  
MASTER OF SCIENCE

Department: Chemical Engineering and  
Nuclear Engineering  
Major: Nuclear Engineering

---

Signatures have been redacted for privacy

Iowa State University  
Ames, Iowa

1974

## TABLE OF CONTENTS

	Page
I. INTRODUCTION	1
II. REVIEW OF LITERATURE	3
III. DESCRIPTION OF ALRR	5
IV. METHOD OF ANALYSIS	13
A. Introduction to KENO	13
B. Modeled Core	14
C. Selection of Cross Sections	34
D. Input Format	35
V. EXPERIMENTAL MEASUREMENTS AND RESULTS	41
VI. SUMMARY AND CONCLUSIONS	51
VII. BIBLIOGRAPHY	56
VIII. ACKNOWLEDGEMENTS	58
IX. APPENDIX A: CROSS SECTIONS ON TAPE	59
A. Available Albedos	59
B. Mixtures	60
C. Elements	61
X. APPENDIX B: CALCULATION OF THE POTENTIAL SCATTERING CROSS SECTION OF THE FUEL MIXTURE	65
XI. APPENDIX C: CALCULATION OF REACTIVITY WORTH AND DEVIATION	66

## LIST OF ILLUSTRATIONS

	Page
Figure 1. Cut away view of ALRR	6
Figure 2. ALRR fuel assembly	8
Figure 3. ALRR control rod poison section	9
Figure 4. Horizontal cross section of ALRR	12
Figure 5. ALRR core configuration - triangular pitch	16
Figure 6. Modeled core configuration	17
Figure 7. Six zones of modeled core region	19
Figure 8. Modeled fuel assembly	22
Figure 9. Modeled control rod	24
Figure 10. Regions used in homogenization process	27
Figure 11. Mixed box orientation - zone 3	31



## LIST OF TABLES

		Page
Table	1. Cuboid arrangement of modeled fuel assembly box	23
Table	2. Box description of modeled control rod	25
Table	3. Volume inventory of reactor materials	28
Table	4. Example of mixture table	30
Table	5. Mixed box formation of zone 3	32
Table	6. Data used for determining length of run	43
Table	7. Effect of varying WTAVG on total histories obtained	46
Table	8. Summary of KENO results and reactor measurements	52

## I. INTRODUCTION

Buffon (1707-1788) (1), is considered by some people to have introduced the first Monte Carlo calculation, the needle problem, which consisted of throwing a needle at random on a surface marked with parallel lines spaced two needle lengths apart. The total throws divided by the number of times the needle hits a line approaches  $\pi$  as the number of trials is increased. Since that time, man's ingenuity and fast computers have made the Monte Carlo method a useful tool in neutron transport problems.

In early attempts to use Monte Carlo methods for reactor calculations, the limited memory capacity of computers was the cause of its demise. It was not practical to handle the large volume of cross section data needed and also, point cross-section data were not readily available. With the development of large memory fast computers and adequate cross-section libraries, the Monte Carlo method has become an important analysis technique. The three dimension capability has made the Monte Carlo calculation one of the most exact at the present time. Computer time appears to be a limiting factor since a Monte Carlo result is exactly correct only when an infinite number of independent estimates of a given result have been obtained.

The majority of the existing diffusion and transport codes are limited by the following three items. First, the

codes are, at best, only two dimensions which means approximations must be made. Secondly, the codes are usually based upon the assumption that an equilibrium distribution of neutrons is present at the start of an analysis, which makes the study of time-dependent situations rather difficult. Thirdly, most codes are capable of handling only few group cross sections. The Monte Carlo procedure is equivalent to obtaining an exact solution of the Boltzman transport equation. In theory, the Monte Carlo method eliminates the deficiencies of other systems mentioned above. In reality, the Monte Carlo system is still limited by computer storage and statistics. As a result of the latter, a balance must be achieved between statistics and computer costs.

This thesis describes how the Ames Laboratory Research Reactor (ALRR) core region was modeled and the input required to be able to utilize the Monte Carlo computer code KENO (2) for criticality calculations. Reactivity calculations in terms of k-effective (k-eff) were made for various reactor configurations and compared to measurements made on the actual reactor.

## II. REVIEW OF LITERATURE

In 1957 Kalos and Wilf (3) reporting on the uses of Monte Carlo calculations in solving reactor problems, state that they may eventually be used for complete reactivity calculations. Since that time, considerable work has been done to make the Monte Carlo method feasible for multigroup criticality analysis.

Rief and Kschwendt (4) have shown that detailed Monte Carlo analysis for fast reactor studies can be carried out with sufficient accuracy to be comparable with equivalent  $S_n$  and  $j_n$  calculations. Mendelson (5) reports using the O5R Monte Carlo computer code (6) to investigate the ability to compute the criticality of thermal reactors by analyzing three simple critical assemblies. The results of these analyses show that a precision of 0.5% to 0.8% in the eigenvalue is obtainable. The majority of Monte Carlo work has been in computing the criticality of fast assemblies, while the application to thermal systems has been somewhat limited. Woodcock, et al. (7), have developed the GEM Code (8) which has been used for Monte Carlo neutronics calculations in reactors. The O5R code and the GEM code are the forefathers of the KENO code used in this analysis.

At the present time, the KENO code is the main code used in industry for performing criticality analyses involving safety questions on fresh fuel storage, spent fuel storage



and safety analyses of batch fuel processes. Its application to a criticality analysis of a thermal reactor is, perhaps, stretching its capabilities; but it yields a tool that can be used to obtain reactivity worths of various core changes with the control rods included in the calculations. Previous analyses of the ALRR core by J. C. Crudele (9) using the diffusion code, EXTERMINATOR-2 (10), was limited to R-Theta geometry with the control rods fully withdrawn. Many calculations that can be made are affected by the location of strong absorbers such as the control rods. The KENO code can handle strong absorbers which gives it an extreme advantage over the diffusion code.

## III. DESCRIPTION OF ALRR

The ALRR Hazards Report (11) describes the reactor as a heterogeneous arrangement of highly enriched uranium-aluminum fuel assemblies using aluminum as a structural material and heavy water as moderator, reflector and main coolant. Figure 1 shows a cutaway view of the reactor. The area of interest for this report is the center-most portion of this view, that is, the region having sides and bottom defined by the thermal shield vessel and top defined by the bottom of the lower top shield plug. Major items in this region are the thermal shield vessel, H<sub>2</sub>O reflector, the D<sub>2</sub>O vessel, the D<sub>2</sub>O moderator, experimental facilities, control rods, fuel assemblies and aluminum structural material.

The major vessel is the D<sub>2</sub>O vessel. It is a cylindrical vessel having a wall thickness of approximately 0.5 inches. It is 6 feet high with a diameter of 5 feet. The reactor core is located in the center of this vessel and is in the form of a right circular cylinder approximately 24 inches high and 32 inches in diameter. This provides a D<sub>2</sub>O reflector region in the vessel of approximately 15 inches on the sides, 30 inches on the top and 18 inches beneath the core region. The core region is composed of twenty-four fuel assemblies and six control rods plus additional D<sub>2</sub>O moderator. The fuel assemblies are arranged in three concentric circles, six assemblies on a 5.25 inch radius, six

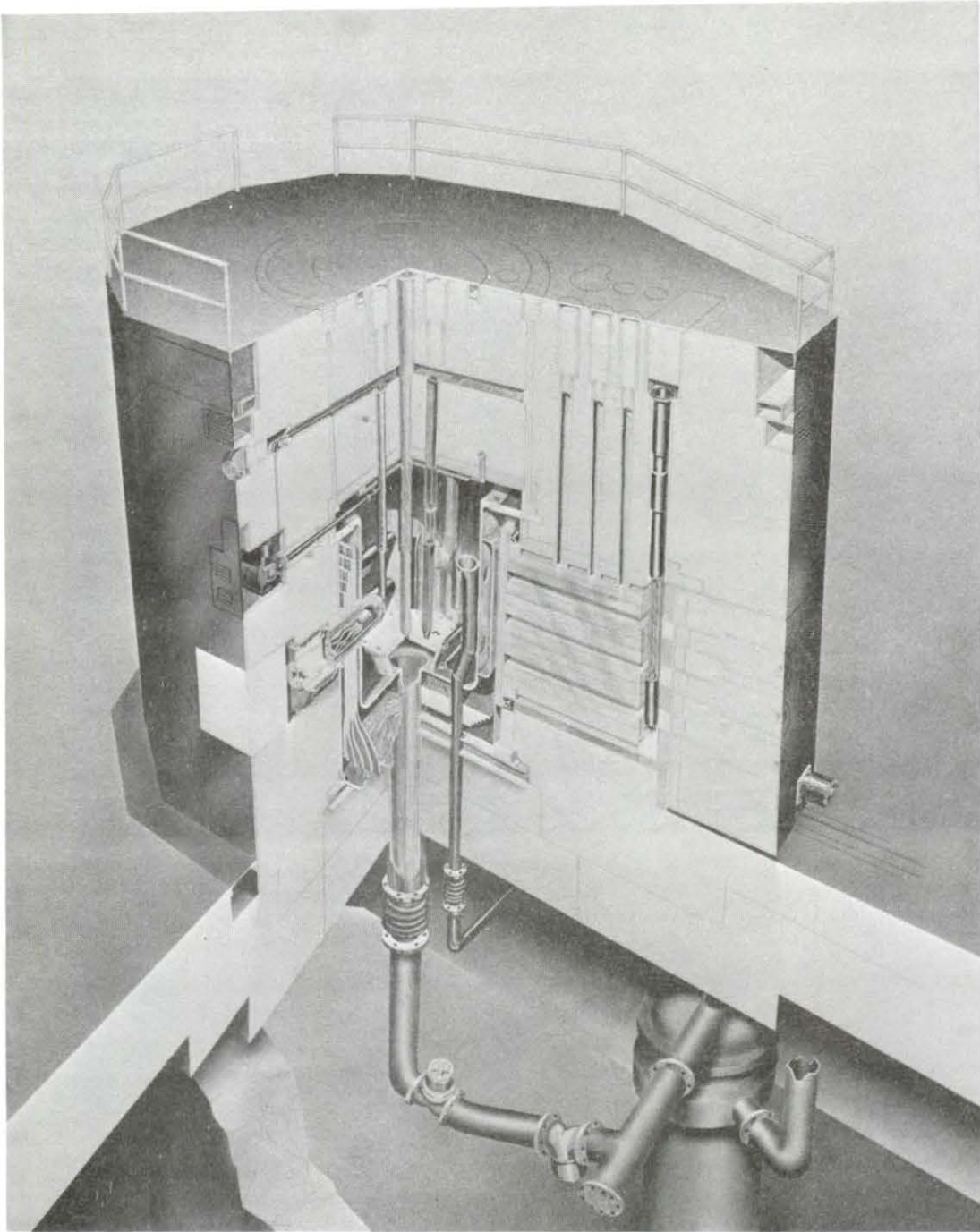


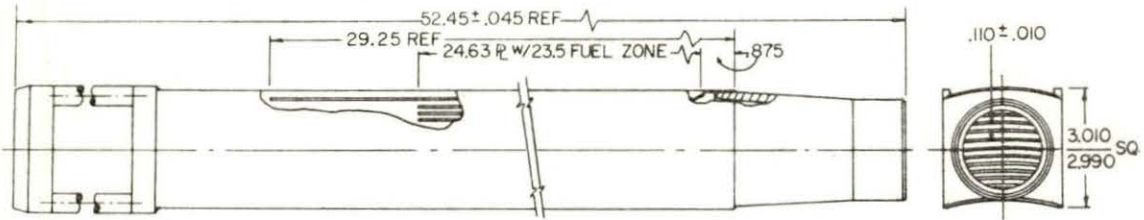
Figure 1. Cut away view of ALRR



assemblies on a 10.5 inch radius and the remaining twelve assemblies are located on a 13.89 inch radius. The control rods also form a circle with their centers on a 9.09 inch radius. The fuel assembly itself is composed of seventeen curved plates. Fifteen of these are fuel bearing plates made up of a layer of uranium-aluminum alloy, clad on each side with a layer of aluminum, each of the three layers being 0.020 inches thick. The remaining two plates are composed of aluminum only and serve as side plates. These seventeen plates are held together by two end plates. This arrangement forms a 3 inch square box and allows .110 inches between plates. There are approximately 11.33 grams of U235 per plate resulting in an average of 170 grams U235 per assembly. The active fuel length is 23.5 inches. The total length of the completed fuel assembly, including hold-down extension bar and transition nozzle is approximately 52.5 inches. Figure 2 shows a cross-section and a vertical section of a fuel assembly.

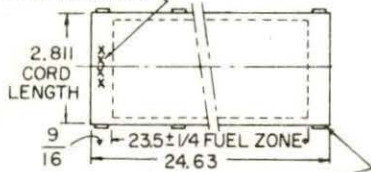
The control rod which is shown in Figure 3 has a 28 inch length of travel from its full in position to 100% withdrawn. The poison section is composed of a cadmium cylinder which has an internal radius of 1.37 inches and a cadmium thickness of 0.060 inches and a length of 19.87 inches. The cadmium is encased in stainless steel 20.5 inches long and .065 inches thick which results in an OR of 1.5 inches and an IR of 1.31



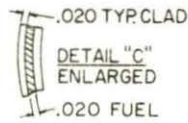
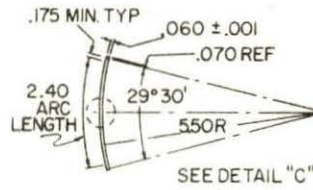


FUEL ELEMENT ASSY

INSCRIBE SERIAL NUMBER HERE  
 1/8" HIGH MAXIMUM



BREAK ALL SHARP  
 EDGES .015R



FUEL ELEMENT PLATE DETAIL

Figure 2. ALRR fuel assembly

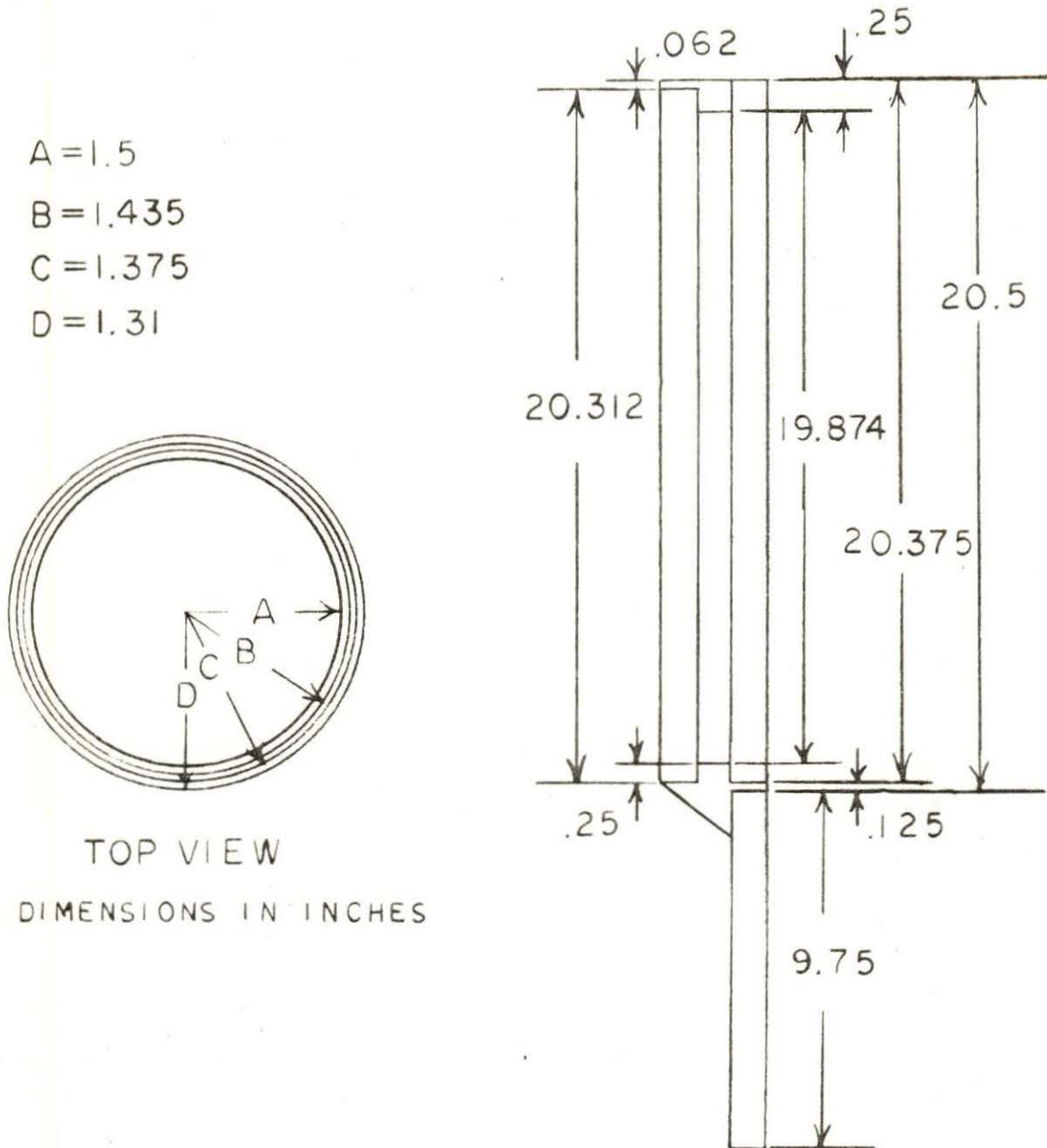


Figure 3. ALRR control rod poison section

inches. At the bottom of the poison section is a stainless steel follower which is .065 inches thick, 9.75 inches long and has an OR of 1.50 inches. These rods have an armature attached to the poison section and by manipulating a rack and pinion magnet drive, the magnet can be lowered onto the armature and by energizing the magnet, the control section can be withdrawn from the core. By de-energizing the magnet, the poison section will free fall into the core.

The major structural components located in the  $D_2O$  vessel are the upper and lower grid plate, fuel assembly guide tube, fuel assembly hold down plug,  $D_2O$  return tubes,  $D_2O$  overflow tube, control rod guide tubes, and  $D_2O$  dump tube. Also located in the  $D_2O$  vessel are six vertical irradiation facilities, nine horizontal irradiation facilities and two rabbit tubes along with two grazing tubes that also pass through the vessel. There are additional facilities but they are not considered large enough to cause significant voids in the reflector or moderator.

The  $D_2O$  vessel is enclosed by the thermal shield vessel which is an aluminum tank, 8 feet in diameter. This provides an 18 inch annulus between vessels, which is composed of  $H_2O$  and six 1 inch stainless steel plates. This system provides the final protection for the biological shield. The thermal shield does not encircle the  $D_2O$  vessel completely. A small portion of this outer reflector is penetrated by the thermal

column. Figure 4 shows a horizontal cross section of the reactor and the relationship between the major components.

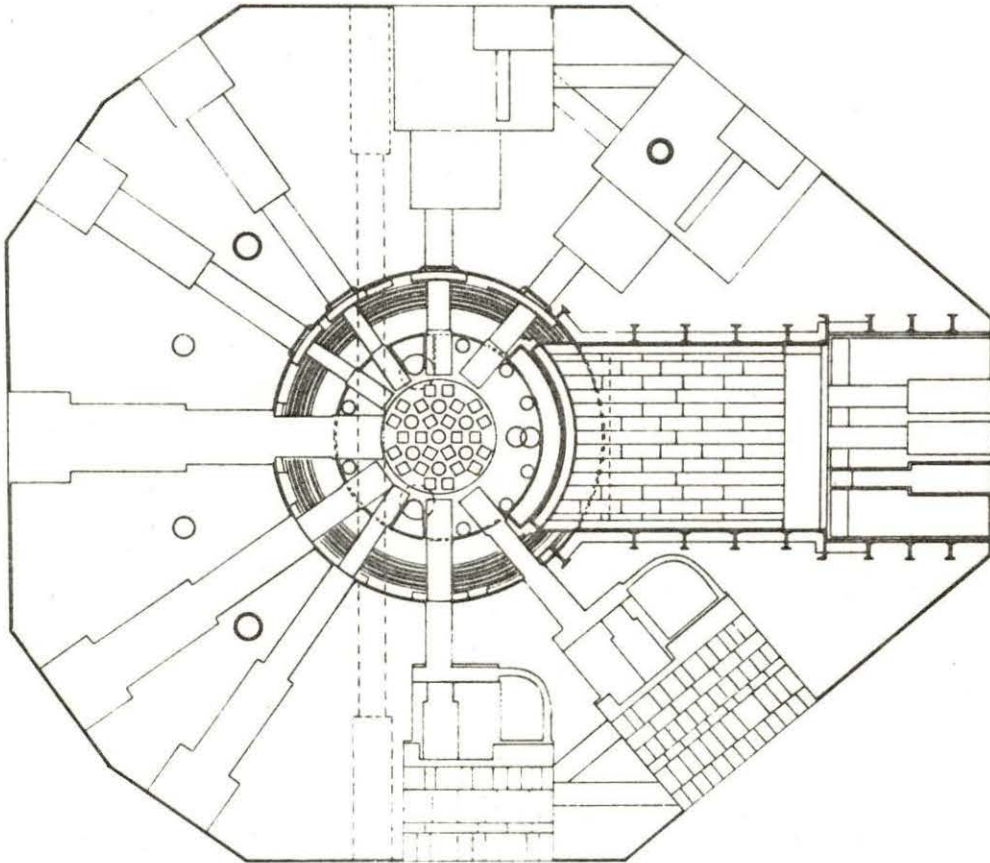


Figure 4. Horizontal cross section of ALRR



#### IV. METHOD OF ANALYSIS

##### A. Introduction to KENO

The development of KENO, a multigroup Monte Carlo criticality program, resulted from the need to calculate the criticality condition of a proposed prompt-burst reactor design of cylindrical geometry. It was not considered realistic to homogenize the system in order to reduce the geometry to two dimensions for calculational purposes. Consequently, a three dimensional criticality code was required. The existing Monte Carlo codes GEM and O5R were considered, but were not deemed adequate for various reasons.

In the case of the O5R program, the lack of adequately checked point-set cross sections for a number of materials was one of the reasons for not using it, but it was noted that at one point in its history, the O5R program had been used with six-energy-group Hansen-Roach (12) neutron cross sections for uranium. This led to modifying the O5R code to use the existing sixteen-energy-group Hansen-Roach (12) cross sections that were available for a number of nuclei. This combination yielded results which were in excellent agreement with experimental data. The O5R code was further modified to allow easier geometry description of complex units and arrays of units. The geometry package developed to achieve this was patterned after the geometry package of the GEM Monte Carlo program. The resulting package, KENO, was a very rapid pro-

gram which could accurately determine the criticality condition of systems of fissile materials.

In order to determine the critical condition of a fissile system, KENO determines k-effective where k-eff is defined by the following expression:

$$k\text{-eff} = \sum_{j=1}^{\text{NPB}} \sum_{i=1}^{\text{NCOLL}} \text{WT}_{ij} \frac{\gamma \Sigma_f}{\Sigma_t} / \sum_{j=1}^{\text{NPB}} \text{WT}_{0j}$$

NPB is the number of neutrons per batch

NCOLL is the number of collisions for each neutron

$\text{WT}_{ij}$  is the statistical weight of the  $j$ th neutron at the  $i$ th collision

$\gamma$  is the average number of neutrons born per fission

$\Sigma_f$  is the macroscopic fission cross section

The method used to accomplish this calculation is summarized in the KENO program manual CTC-5 (2).

#### B. Modeled Core

The KENO program allows easy description of three-dimensional systems composed of cylinders, spheres and cuboids (rectangular parallelepipeds) in any order with only one restriction: each geometrical region must be described as completely enclosing all regions interior to it. In

conjunction with this, boundaries of the surfaces of regions may be shared but they must not intersect. This implies that the entire volume between two sequential geometrical surfaces contains only one mixture. If multiple units are combined to form an array, as in the case of describing the complete core, then the outer surface of each unit must be a cube or cuboid. If the total array is surrounded with a reflector region, an initial cube or cuboid must be described which exactly encloses all units in the array. The reflector region is then described relative to this core boundary.

The ALRR core was modeled in such a fashion that the original triangular pitch configuration shown in Figure 5 was converted to the x, y array shown in Figure 6. This was done by rotating sixteen of the twenty-four fuel assemblies, 30 degrees, about their centers. This results in eight columns of fuel assemblies all aligned with the same x, y orientation and three columns of control rods. These columns overlapped some of the fuel assembly columns in the x direction but not in the y direction. The next step was to expand the x, y grid system in the y direction until none of the columns of fuel assemblies or control rods overlapped, since the rules prohibit the intersection of boundaries. The amount of displacement of the columns ranged from .37 inches to 1.94 inches. Due to the angular arrangement of the assemblies prior to their rotation, the displacement of the



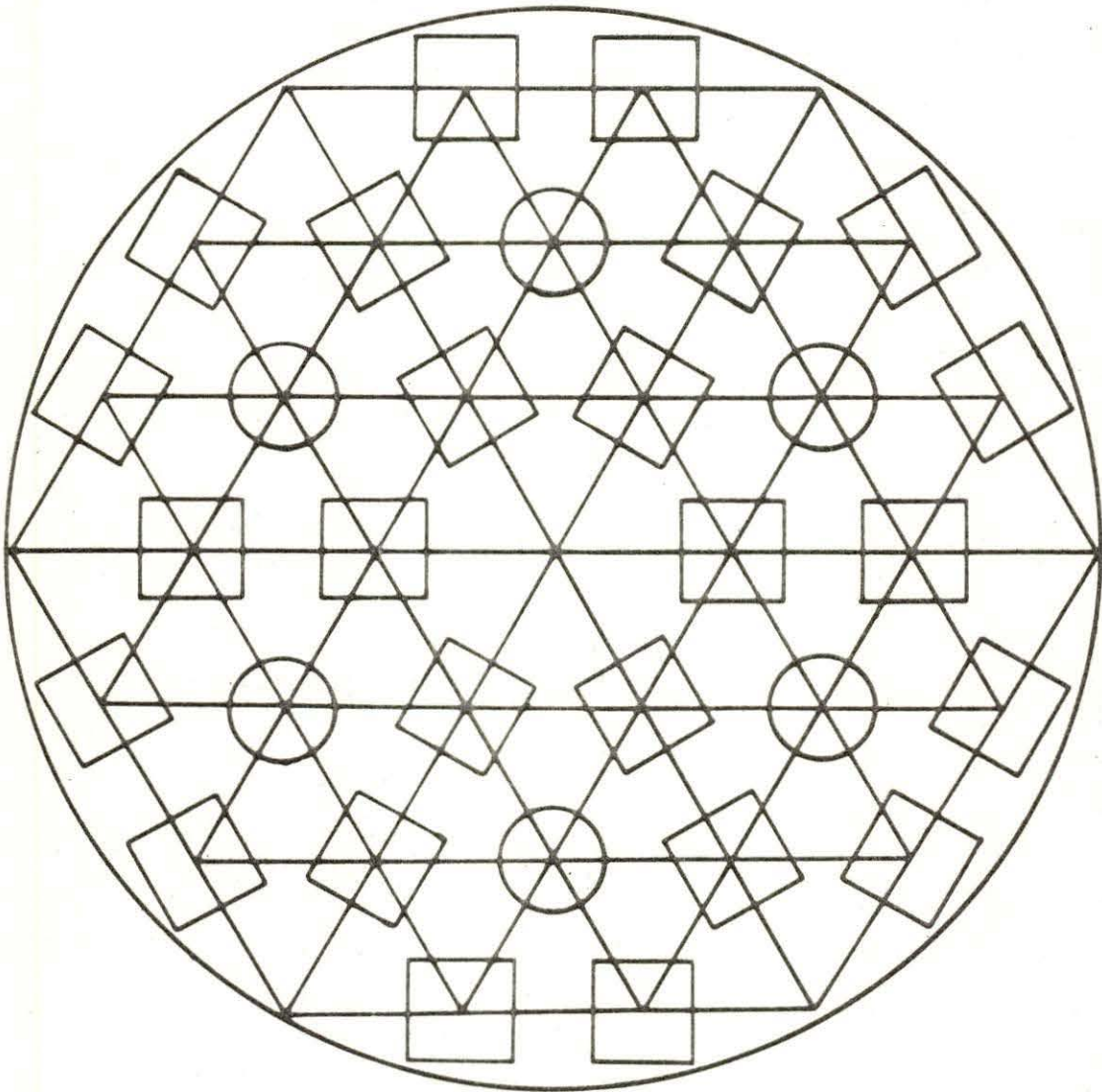


Figure 5. ALRR core configuration - triangular pitch

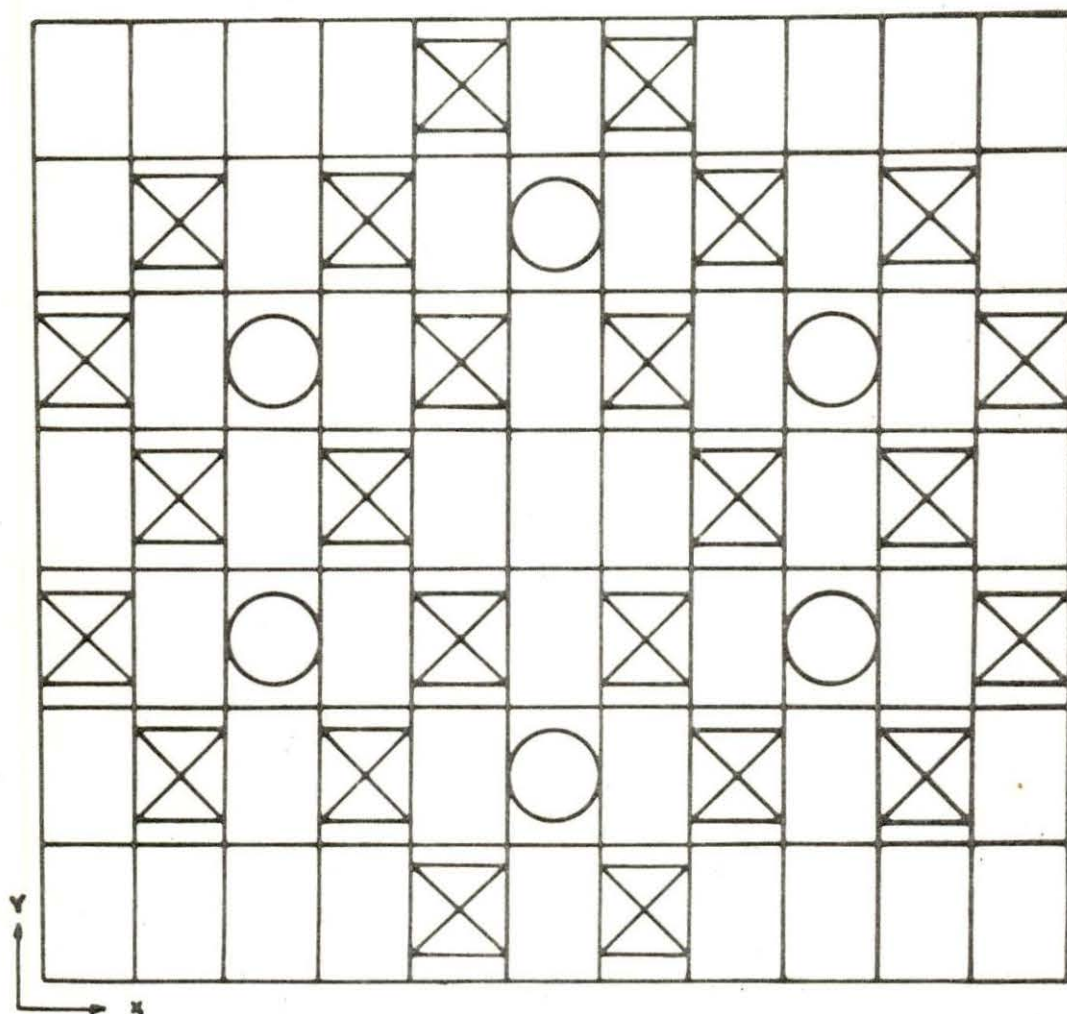


Figure 6. Modeled core configuration

columns resulted in a core boundary of 33 inches by 31.5 inches instead of a 32 inch diameter circle. The x, y grid is formed by boxes 3 inches by 4.5 inches in the form of an 11 by 7 array as shown in Figure 6. The height of this x, y array is approximately 62 inches and is divided into six zones. The height of the individual zones is a variable but all box heights are equal within a particular zone. The zones are used to terminate a particular box so that the geometric arrangement is constant in the z direction. For example: the control rod is composed of a poison section and a dashpot section, the normal transition point being the intersection of these pieces. It is not permissible to describe the complete control rod in a single box due to the change in material in the z direction.

For the case where the control rods are 40% withdrawn, the six zones are divided as follows and are shown in Figure 7. Starting at the top of the plenum, the first zone is up to the base of the meat in the fuel plate of a fuel assembly. This level is composed of boxes 3 x 4.5 x 6.38 inches high and the mixture included is homogenized D<sub>2</sub>O and aluminum. The second zone is composed of boxes containing moderator only and boxes containing a portion of a fuel assembly plus moderator. These boxes have a height of 8.2 inches. The third zone contains boxes which describe a fuel assembly section, control rod follower and moderator. The height of this

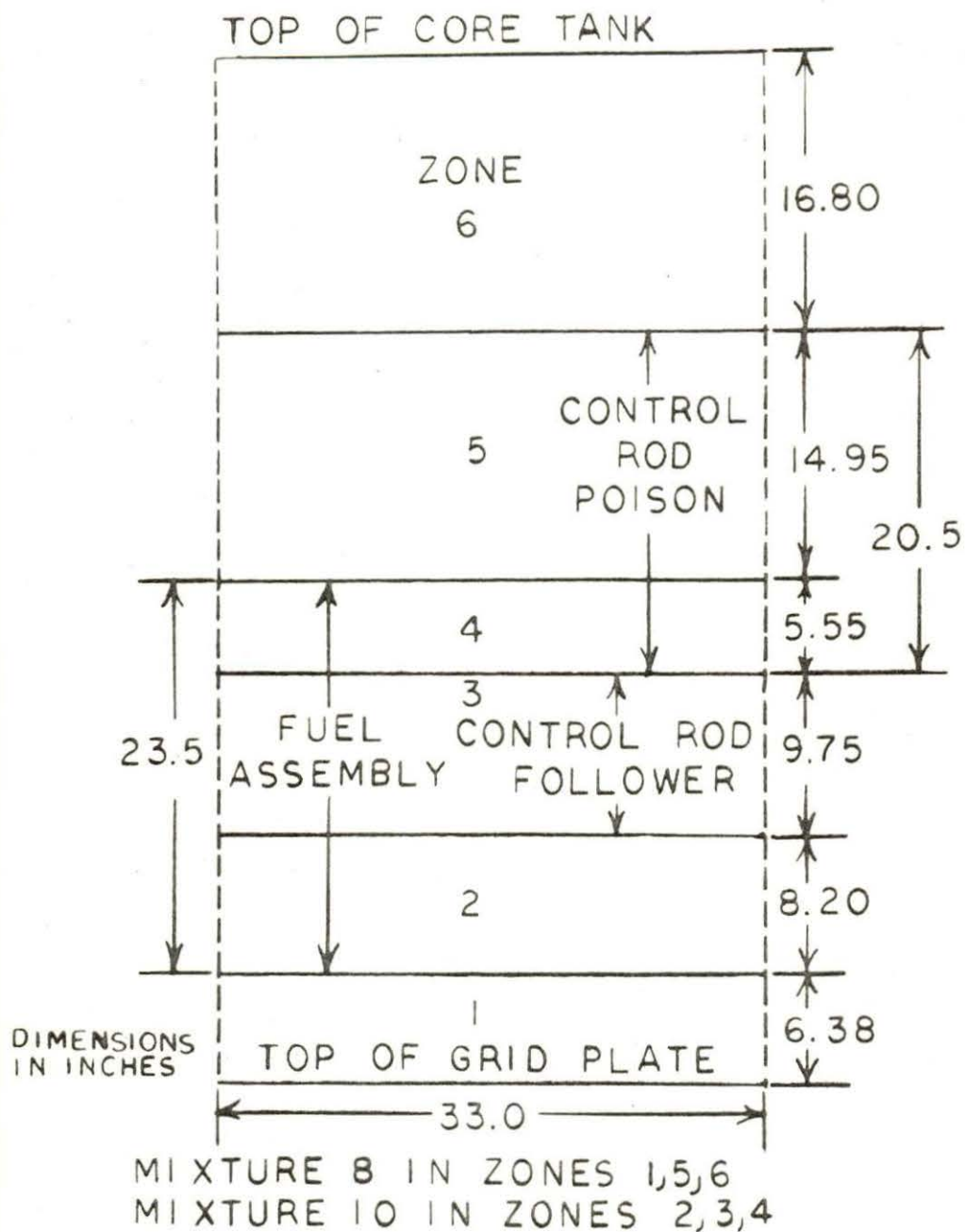


Figure 7. Six zones of modeled core region



zone is based on the length of the follower which is 9.75 inches. The fourth zone is based on the remaining section of the fuel assembly which is 5.55 inches. The other boxes in this zone contain a section of control rod or moderator only. The fifth zone contains two box types, one containing the remaining section of control rod and the other being just moderator. This zone is 14.95 inches high. The last zone is composed of boxes of moderator only and is used to fill the remaining core, with moderator, to the top of the D<sub>2</sub>O vessel. The twelve box types do not imply twelve different core materials to be described but rather indicates the need for multiple boxes to completely describe a particular item. For example, due to the number of zones, it required three box types to describe the fuel assembly with the only difference between boxes being the height.

At this point, an array 11 x 7 x 6 has been described made of twelve box types all 3 x 4.5 inches in the x, y field and of six different heights in the z field. These twelve box types can be divided into four groups: fuel assembly, control rod and two groups of moderator.

Since a complete three-dimensional description of the reactor would require a great deal of computer storage, a compromise was reached where the major components were described in rather close detail while the structural material was accounted for by homogenizing it with the moderator. Of

the four groups of box types, the fuel assembly and control rod fall into the major component class and the following paragraphs are used to describe their geometric layout in the x, y field, while in the case of the moderator box types, the geometry is completely described by the 3 x 4.5 inch dimensions. The only thing remaining is to define the mixture contained in the different types.

The initial step in describing the fuel assembly was to reduce its complexity by only taking into consideration the fuel zone. Secondly, the slightly curved plates were straightened so that the assembly could be described in terms of a series of cuboids. Figure 8 shows the resulting box whereby starting with the middle fuel plate and adding cuboids as shown in Table 1, the fuel assembly is described in the x, y plane. In this case, the fuel and the aluminum clad were homogenized to form the fuel plate thereby reducing the number of cuboids needed to describe the assembly.

Figure 9 shows the box type describing the poison section of the control rod with Table 2 indicating the dimensions, geometry and material arrangement. As with the fuel plate, the cadmium and stainless steel clad were homogenized. One section of the control rod differs from the other two in that it describes only the follower which is made of stainless steel and has an inner radius of 1.435 inches while the outer radius is 1.5 inches.

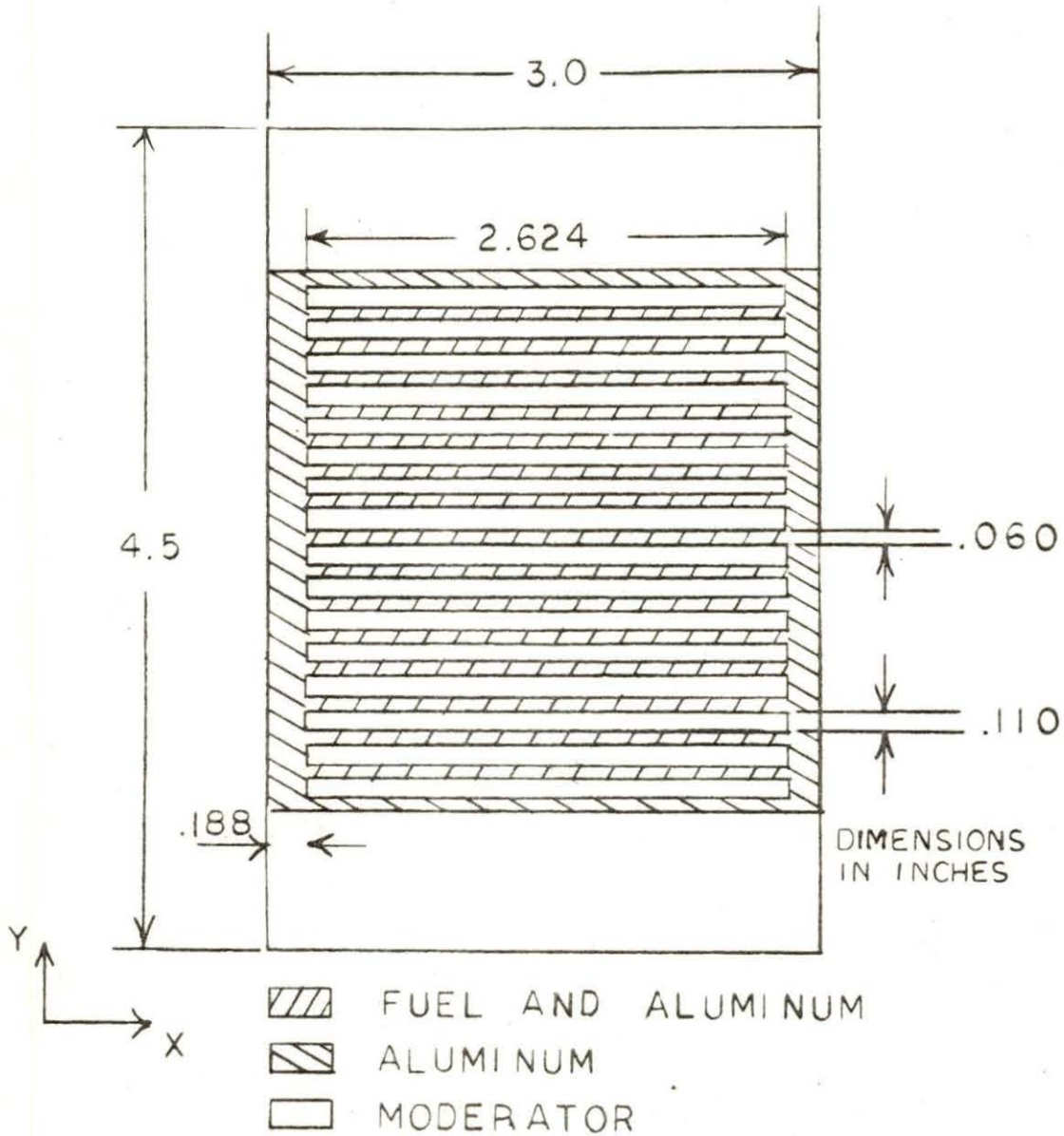


Figure 8. Modeled fuel assembly

Table 1. Cuboid arrangement of modeled fuel assembly box

Cuboid Number	Material	y-dimension (inches)	x-dimension (inches)
1	fuel + aluminum	0.06	2.624
2	moderator	0.28	2.624
3	fuel + aluminum	0.40	2.624
4	moderator	0.62	2.624
5	fuel + aluminum	0.74	2.624
6	moderator	0.96	2.624
7	fuel + aluminum	1.08	2.624
8	moderator	1.30	2.624
9	fuel + aluminum	1.42	2.624
10	moderator	1.64	2.624
11	fuel + aluminum	1.76	2.624
12	moderator	1.98	2.624
13	fuel + aluminum	2.10	2.624
14	moderator	2.32	2.624
15	fuel + aluminum	2.44	2.624
16	moderator	2.56	2.624
17	aluminum	2.78	3.000
18	moderator	4.50	3.000



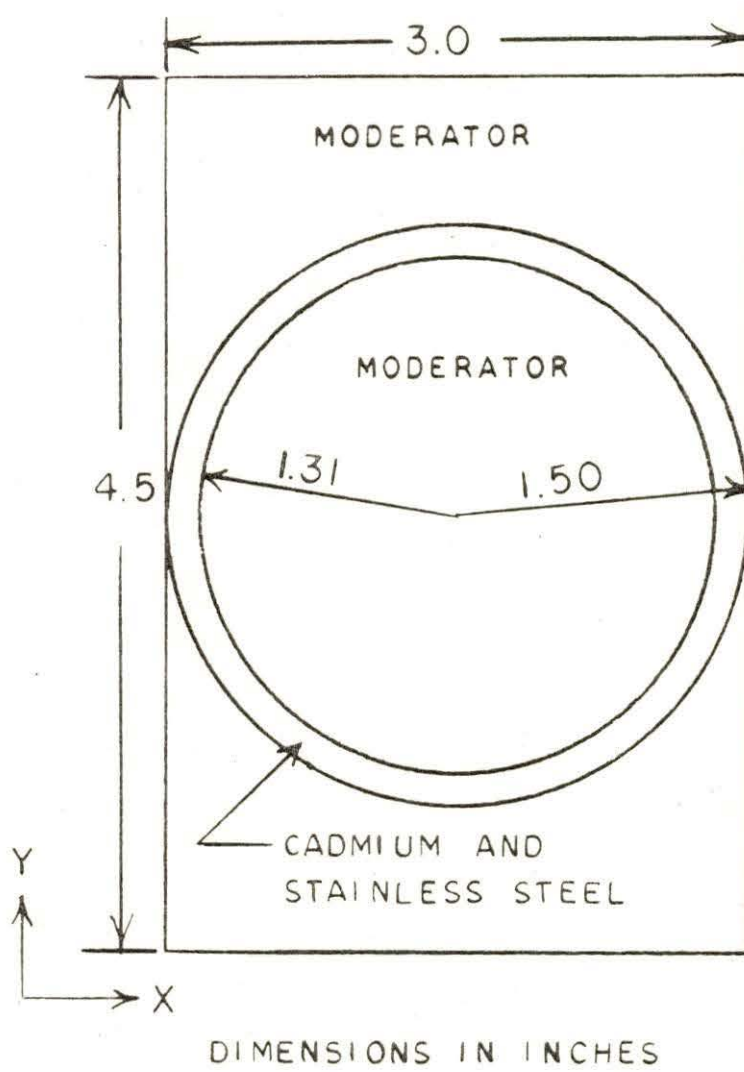


Figure 9. Modeled control rod

Table 2. Box description of modeled control rod

---

Item Number	Geometry	Material	x-dimension or Radius (inches)	y-dimension (inches)
1	Cylinder	Moderator	1.31	--
2	Cylinder	Stainless Steel and Cadmium	1.50	--
3	Cuboid	Moderator	3.00	4.50

---

The moderator boxes are all 3 x 4.5 inch boxes, the difference between them being due to the amount of structural material located in a particular zone. In this case, for zones 2, 3 and 4, the moderator is pure  $D_2O$  and in this section of the core, the control rods and fuel assemblies are completely described. In zones 1, 5 and 6, the moderator is homogenized with the total volume of structural material located in these regions. Figure 10 shows the regions the core was broken into in determining the  $D_2O$  and structural material inventory. Table 3 gives the volume of moderator and structural material in the various regions.

Now that each box type has been described in terms of a geometric arrangement, it is necessary to instruct the computer what material or mixture to place in each respective box and how to arrange the boxes so that they represent the core region.

In order to accomplish the first item, the user must establish a mixing table. This table can be made up of items listed in Appendix A, Section A, which lists the description of albedo functions available. Section B lists the mixtures whose cross sectional data are available, such as stainless steel, water, etc. Section C lists the elements whose cross-sectional data are available.

In order to form the mixing table, each mixture is numbered sequentially starting with one. Each numbered entry

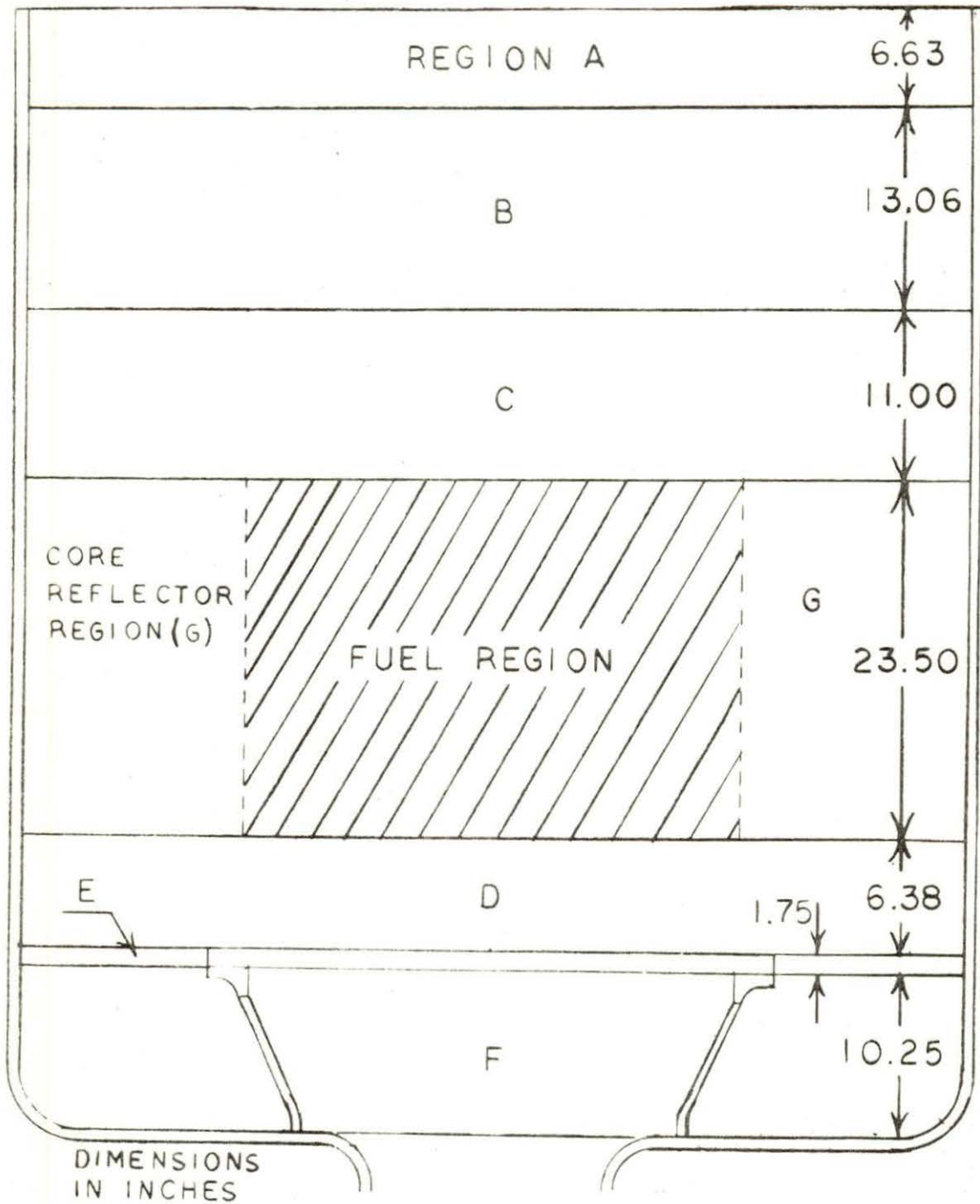


Figure 10. Regions used in homogenization process

Table 3. Volume inventory of reactor materials

Region	Aluminum	Volume (cubic inches) Moderator	Void*
A + B	1380.14	54272.02	--
C	2384.61	28717.16	--
D	1126.08	16911.65	--
E	1643.29	3304.71	--
F	1824.04	26772.99	384.14
G	2658.06	27956.31	11402.16**

\* Voids due to irradiation facilities.

\*\* Total vertical thimble volume included in this region.



may be composed of an individual element, a group of elements, a single mixture from Section B, Appendix A, or finally any combination of the previous. The input nuclide number obtained from Appendix A is entered along with the volume fraction (if the entry is from Section B) or the atomic density (if the entry is from Section C) for each item entered. This is repeated for each numbered mixture until the table includes all the materials described in the core. Table 4 shows an example of a mixing table.

The arrangement of the different box types in each zone is done by considering them as consisting of a three-dimensional matrix of box type numbers, with the box position increasing in the positive x and y directions. To enter boxes into this matrix, a method similar to a Fortran do loop is used, where three sets of three fields are needed. The first entry in each set is the starting point, the second is the ending point and the third entry of each set is the number of boxes by which increases are made. Figure 11 shows the mixed boxed formation of zone three of the core. Table 5 shows the do loop formation of this matrix. It should be noted that the last box type that locates a specific spot is the one that is retained.

Once the core region has been established, the core boundary is entered. The core boundary is a set of dimensions which completely encloses the core matrix. The mixture

Table 4. Example of mixture table

Mixture	Nuclide ID Number	Atomic Density or Volume Fraction
1	1201	6.4934 E -02
1	8100	3.2467 E -02
1	501	2.3000 E -02
2	13100	5.9600 E -02
2	-92504*	4.7908 E -04
2	92845	3.5592 E -05
3	200	1.0000 E -00

\* A negative Nuclide ID number indicates that the fission spectrum for that nuclide will be used.





Table 5. Mixed box formation of zone 3

---

Box Type	X	Y	Z
3	1, 11, 1	1, 7, 1	3, 3, 1
7	5, 7, 2	1, 7, 2	3, 3, 1
7	2, 4, 2	2, 6, 2	3, 3, 1
7	1, 11, 10	3, 5, 2	3, 3, 1
9	6, 6, 1	2, 6, 4	3, 3, 1
9	3, 9, 6	3, 5, 2	3, 3, 1

---

input is represented by a zero which implies a void. All reflector regions are referenced to the core boundary. The reflector was added on in three sections. This allowed the moderator mixture in each of the regions to be different. The first region added was that above the grid plate and outside the core matrix. The next region was that region that contained the grid plate. The last moderator region was the remaining moderator below the grid plate.

For the region above the grid plate, the aluminum structural volume, voids due to experimental facilities, the  $D_2O$  in regions A, B, C, D and the core reflector region shown in Figure 10 were homogenized. The fuel region in Figure 10 is equivalent to zones 2, 3 and 4 of Figure 7. In regions E and F, the  $D_2O$  and structural aluminum were also homogenized. Regions E and F were not combined to prevent dilution of the high aluminum concentration in region E with the low aluminum concentration of region F. This completed the description of the core and moderator. The next item added was the aluminum  $D_2O$  vessel. The remaining item left to describe is the thermal shield.

In order to save computer time, it was decided to use one of the albedos included in the KENO program. The closest approximation was the 12 inch  $H_2O$  differential albedo; but to apply it, the core vessel must be surrounded by a cube or cuboid. Therefore, a cuboid was added with the appropriate

dimensions that allowed it to be tangent at the diameter of the vessel. The mixture added to the corners was light water. The albedo was then added referenced to this outer cuboid. Since the thermal shield surrounds just the sides and bottom of the core, the computer was instructed to apply the albedo to these areas only. This then, completed the model of the reactor. Section D describes in more detail the proper arrangement of these data on computer cards for input to the program KENO.

### C. Selection of Cross Sections

The KENO cross-section library is divided into two parts: the first is a table containing nine items that are mixtures. When using materials from this section, volume fractions are used instead of number density for the value of RHOA on card 5 of the input. This implies that the first table is composed of macroscopic cross sections rather than microscopic, as is the second part of the cross-section library. In both tables, some of the cross sections are either lethargy weighted or fission spectrum weighted. The choice between using lethargy weighted or fission spectrum weighted cross sections was one of trial and error with the final selection based on the combinations that yielded a k-effective closest to one for the case where the control rods were at 40% withdrawn.

In the second section of cross sections, some elements, namely the fuels, have a number of different listings based on the potential scattering cross section of the medium per atom of the reacting element. Once the potential scattering cross section has been calculated, the proper cross section can be chosen from the list. This calculation for the ALRR fuel assemblies is shown in Appendix B.

If neither table has the cross section desired, it is possible to enter the appropriate sixteen-group cross section by cards as demonstrated in Section D on input to KENO. The majority of cross sections listed on tape are from the Hansen-Roach (12) sixteen-group cross section set.

#### D. Input Format

The following is the data guide from the KENO manual for the proper input of data. The information is in the order in which the computer reads the data. The Fortran format required is given along with the nomenclature of each item as it is used in the computer program. Data cards not used in this particular application but listed in the manual, have been omitted here.

Card 1	Time Card	Format (2I10.5)	maximum computer time (in minutes) to be allowed for problem
--------	-----------	-----------------	---



Card 2      Title Card      Format (18A4)      contains title  
only

Card 3      Parameter Card      Format (13I5)

cols 1-5	NBA	Number of generations
cols 6-10	NPB	Number per generation
cols 11-15	NSKIP	Number of generations to be skipped
cols 16-20	NGP	Number of energy groups
cols 21-25	NDS	Number of downscatters
cols 26-30	NMAT	Number of input nuclides
cols 31-35	MATT	Number of mixtures
cols 36-40	NMIX	Number of mixing table entries
cols 41-45	KREFM	Total number of geometry cards. This includes the Core Boundary Card, but not the Box Type cards.
cols 46-50	NBOX	The number of box types
cols 51-55	NBXMAX	# of units in the x direction
cols 56-60	NBYMAX	# of units in the y direction
cols 61-65	NBZMAX	# of units in the z direction

Card 4      More Parameters      Format (14I5)

cols 1-5	NTAPE	The number of input nuclides to be read from tape. If NTAPE > 0, read a KENO cross-section tape. If NTAPE < 0, read a XSDRN cross-section tape.
----------	-------	---



cols 6-10	NXX	specifies albedo options
	NXX =	Albedo ID number
cols 11-15	NSCH	Search type = 0 if no search
cols 16-20	LIST	Applies only to cross-sections read from tape.
	LIST = 0	Do not print input cross-sections
cols 21-25	NOXS	If NOXS = 0, read in new cross- sections
cols 26-30	NTYPST	The type of starting distribution NTYPST = 1 Cosine over array, in fissile material only
cols 31-35	NFLX	NFLX = 1 Fluxes not calculated
cols 36-40	NFDEN	NFDEN = 1 Fission densities will not be calculated

Card 5            Reflector constants            Format (6E10.3)

Note: use negative number for diff. albedo

cols 1-10	REFCST(1)	Reflector const. for +x direction
cols 11-20	REFCST(2)	Reflector const. for -x direction
cols 21-30	REFCST(3)	Reflector const. for +y direction
cols 31-40	REFCST(4)	Reflector const. for -y direction
cols 41-50	REFCST(5)	Reflector const. for +z direction
cols 51-60	REFCST(6)	Reflector const. for -z direction

Card(s) 6    Mixing Table    Format (2I10, E10.4)    Enter only if

NOXS = 0

cols 1-10	KKA	Mixture number
-----------	-----	----------------

cols 11-20 NMA Nuclide ID number

A negative ID indicates that the fission spectrum for that nuclide will be used. Nuclides read from cards are assigned sequential ID numbers starting with 1

cols 21-30 RHOA Number density (atoms/barn-cm)  
there must be NMIX cards 6

Cards(s) 7 Cross Sections From Cards Enter only if  
NOXS = 0 and  
NTAPE < NMAT

Card(s) 7a Title Card Format (17A4,A3,I1)

cols 1-71 XST Nuclide identification

cols 72 IORDER Enter 0 if  $P_0$  component only

Card(s) 7b  $P_0$  cross-section set (two cards per group)

cols 1-12 13-24 25-36 37-48 49-60 61-72

GP1  $\sigma_a^1$   $\gamma\sigma_f^1$   $\sigma_t^1$   $\sigma_{1\rightarrow 1}$   $\sigma_{1\rightarrow 2}$   $\sigma_{1\rightarrow 3}$

GP1  $\sigma_{1\rightarrow 4}$   $\sigma_{1\rightarrow 5}$   $\sigma_{1\rightarrow 6}$

Repeat sequence for groups 2 thru 16

Card(s) 8 Geometry Card and Weights

Card(s) 8a Box Type Card Format (2A4,A2,I6)

cols 1-8 "BOX TYPE" (left adjusted)

cols 11-16 The box number (between 1 & NBOX)  
(right adjusted)

Card(s) 8b Geometry Cards Format (2A4,A2,I6,5E8.0)

cols 1-10	FGEOM	FGEOM may be one of the following and must be left adjusted: CUBE CUBOID, SPHERE, CYLINDER, XCYLINDER, YCYLINDER, HEMISPHERE.
cols 11-16	MAT	Mixture number
cols 17-24	XX(1)	Radius for sphere, cylinders, hemisphere +x dimension for cube, or cuboid
cols 25-32	XX(2)	-x dimension for cube or cuboid, +z for cylinder, +x for xcyylinder, +y for ycyylinder
cols 33-40	XX(3)	+y dimension for cuboid -z for cylinder, -x for xcyylinder, -y for ycyylinder
cols 41-48	XX(4)	-y dimension for cuboid
cols 49-56	XX(5)	+z dimension for cuboid
cols 57-64	XX(6)	-z dimension for cuboid
Card(s) 8c	Weight Cards	Use blank card for default values.

Note: repeat 8a,8b,8c, sequence until NBOX box types have been described

Card(s) 8d	Core Boundary Card	Format (2A4,A2,I6,6E8.0)
cols 1-8	FGEOM	"CORE BDY" (left adjusted)
cols 9-16	MAT	Zero usually (right adjusted)
cols 17-24	XX(1)	+x dimension of cube or cuboid

cols 25-32	XX(2)	-x dimension of cube or cuboid
cols 33-40	XX(3)	+y dimension for cuboid
cols 41-48	XX(4)	-y dimension for cuboid
cols 49-56	XX(5)	+z dimension for cuboid
cols 57-64	XX(6)	-z dimension of cuboid

Card(s) 8e Weight Card            Use blank card for default values.

Card(s) 8f Reflector Geometry Cards    See cards 8b.

Card(s) 8g Weight Cards            See cards 8c.

Note: repeat 8f,8g until reflector region has been completely described.

Card(s) 9 Mixed Box Orientation Cards

Format [I2,3(3X,I4,1X,I4,1X,I4),1X,A1]

Note: last data card uses nonblank character in column 55.



## V. EXPERIMENTAL MEASUREMENTS AND RESULTS

Once the reactor core was modeled, KENO was run on the Iowa State University IBM computer, Model 360/65, for a number of different conditions. Initially, runs were made to establish the effect of using lethargy or fission spectrum weighted cross sections. Runs were also made to establish the effect of homogenizing various sections of the core. The only criteria used to judge the effect of these runs was based upon the fact that the actual reactor critical condition for a twenty-four fuel assembly core was obtained with a control rod bank position of 40% withdrawn. Therefore, runs that yielded a k-effective closest to one were judged to be the proper selection. The final selection of input data resulted in a k-eff of  $1.04107 \pm .00556$  for 22275 neutron histories with 275 neutrons per generation. This final arrangement consisted of using the fission spectrum weighted light water cross section in the fuel region and the lethargy weighted cross section in the moderator regions shown in Figure 10. The value obtained implies that with the control rods 40% withdrawn, the reactor is super-critical. In criticality safety calculations (13) using KENO, a value within the range of  $-3\% \Delta k/k$  of a k-eff of 1.0 is considered to be critical. Taking this into consideration along with the fact that there is no temperature compensation for the cross-section data used, it was felt that the value of (+3.95

$\pm .53\% \Delta k/k$  was a reasonable value to establish as a base run for future critical measurements.

The next question that was considered was should the computer run be one long run or should a number of shorter runs be made, varying the number of neutrons per generation for each run and then summing the data from all runs. The reason behind this question was due to the fact that the final answer of one long run would be based upon one continuous random sequence and only one initial source distribution. The data obtained from multiple runs, varying the neutrons per generation for each run, would reflect different random number sequences and, consequently, different initial source distributions. Statistically, the results should be equal, assuming infinite computer time. Since it was relatively easy to vary the random number generation sequence, which is accomplished by varying the number of neutrons tracked per generation, an attempt was made to answer the question, by making three short runs and comparing the results with the one long run. Table 6 shows the data used where set #1 is the one long run and set #2 is three separate short runs. Applying equation one to the data of set #2 yields

$$\text{EQ. 1} \quad k\text{-eff} = \frac{\sum k\text{-eff}}{3} \pm \frac{\sqrt{\sigma_1^2 + \sigma_2^2 + \sigma_3^2}}{3}$$

Table 6. Data used for determining length of run

---

Set	k-eff	Sigma	Neutrons per Generation	Run Time (Hours)	Total Histories
1	1.04107	.00556	275	1.5	22275
2	1.03658	.01463	300	0.5	6600
	1.02573	.00831	325	0.5	6500
	1.04147	.01010	360	0.5	6480

---

a k-eff of  $1.03459 \pm .00654$ . If the data of the second set are further broken down and analyzed by finding the average k-eff for the 63 generations which composed the 19,580 histories and the standard deviation of the average is calculated using equation two, the results obtained are an avg. k-eff =  $1.03443 \pm .00670$

$$\text{EQ. 2. } \sigma = \frac{\sum (k\text{-eff}_i - \bar{k\text{-eff}})^2}{\text{number of generations}}$$

$k\text{-eff}_i$  being the individual k-effective of each generation and  $\bar{k\text{-eff}}$  is the mean. It is observed that both methods of analyzing the data of the second set are in close agreement.

Upon comparing the data of the two methods, it was observed that the magnitude of the value of reactivity worth obtained by subtracting the two sets of data was the same relative magnitude as the deviation of each set. Therefore, it was concluded that either method was suitable and for convenience, all runs would be single runs rather than the multiple runs.

During the execution of the program, absorption of neutrons is not allowed. Rather than absorption, at each collision point of a neutron tracking history the weight of the neutron is reduced by the absorption probability. When the neutron weight has been reduced below a specified point



for the region in which the collision occurs, Russian roulette is played to determine if the neutron's history is to be terminated at that point or if the neutron is to survive with an increased weight. There are three specified points which are entered into the program; these being WTLOW, WTAVG and WTHIGH. If a neutron's weight increases above the WTHIGH value, it is split into two neutrons, each with one-half the weight. The probability of survival when Russian roulette is played depends upon the values chosen for WTLOW and WTAVG. The justification for the values used for these weights is based upon the number of neutrons tracked during a fixed amount of computer time. It is possible to enter user supplied weights or use those suggested in the code. Therefore, a short test was run to see if the default values were suitable for this core configuration. Table 7 shows the results of these tests and illustrates that the default values were a proper selection. WTAVG is related to WTLOW and WTHIGH by WTAVG times three or divided by three; hence, only WTAVG is listed in the table. Also, the weights were varied in the two main regions of concern, the fuel region and the moderator region.

Since a differential albedo was used to approximate the thermal shield, a computer run was made to determine the reactivity effect of this model and compare the reactivity worth obtained with that obtained from actual reactor meas-

Table 7. Effect of varying WTAVG on total histories obtained

Case	WTAVG	Region	Histories
1	0.5* 0.5*	fuel moderator	5100
2	0.3 0.5	fuel moderator	3600
3	0.3 0.7	fuel moderator	3600
4	0.25 0.3	fuel moderator	3000

\* Default values.

urements. Since the base run was available, a run was made without the albedo present and the cuboid surrounding the core tank, which is normally filled with light water, declared a void. This run resulted in a  $k$ -eff of  $1.01993 \pm .00592$ . Using this value and the base run information, the reactivity worth due to the addition of the albedo is  $(1.99 \pm .79)\% \Delta k/k$ . The actual measured value obtained at the time of the initial criticality testing was  $1.48\% \Delta k/k$ . Therefore, the albedo package was considered an adequate representation of the thermal shield.

After these initial runs were completed, another series of computer runs were made so that the code could be further checked out by comparing values determined by the code with values of measurements obtained from actual reactor experiments. These measurements consisted of control rod worths, fuel assembly worth, converter assembly worth and  $H_2O$  filled fuel assembly worth. The following paragraphs will discuss each of the above experiments.

Control rod worths are measured after every refueling at ALRR. The method used is the "rod drop" technique. This is a derivation of the integrated count method of control rod calibration and utilizes one-group, space-independent, zero-power kinetic theory to calculate the behavior of a reactor following a step change in reactivity. This method is applicable to changes in reactivity up to  $10\% \Delta k/k$ . The worth of

each of the six rods is measured individually and then summed, applying a rod shadow factor, in order to obtain the total worth of all rods. The results of the June, 1973, measurements gave a total control worth of  $27.69\% \Delta k/k$  and a reactor shutdown margin of  $14.86\% \Delta k/k$ . Utilizing the KENO code, runs were made for the case with the control rods 100% withdrawn and for the control rods fully inserted. The values of  $k$ -eff are as follows: for the rods full in,  $k$ -eff =  $.87034 \pm .00669$  and for the rods full out,  $k$ -eff =  $1.14864 \pm .00762$ . These values result in a total rod bank worth of  $(27.84 \pm 1.03)\% \Delta k/k$  with a shutdown margin of  $(14.90 \pm 0.78)\% \Delta k/k$ . These values were based on a minimum of 13500 neutron histories.

The reactor measurements of the reactivity worth of a fuel assembly, converter assembly and  $H_2O$  filled fuel assembly were done using a cold, clean core and zero power. The procedure used to obtain the reactivity worth of an item will be described for the fuel assembly. The procedure is essentially the same for the other items.

Starting with a new core of twenty-four fuel assemblies, the reactor was taken just critical with the control rods in a six rod bank. The rod bank position was recorded along with core temperature and other data. The control rod configuration was then changed to a five rod bank with the regulating rod at 75% withdrawn, maintaining the reactor just



critical. Pertinent data was recorded and the reactor shut down. The fuel assembly selected to have its reactivity worth measured, was removed from the core using the appropriate procedures. Upon its removal, another zero power run was made, utilizing a six rod bank and then the five rod bank as determined previously, adjusting for criticality with the regulating rod, recording the rod positions and other data. Utilizing the control rod positions obtained for all four runs and the previously obtained control rod worth calibration curves, the fuel assembly worth can be determined. Using the data from the two six-rod bank runs, the worth of the single fuel assembly is just the difference in reactivity worth of the two six-rod banks correcting for temperature differences between runs. Utilizing the data from the remaining two runs, the worth of the single fuel element is just the reactivity worth represented by the difference in the regulating rod position for the two runs since the five-rod bank is the same for both runs. A correction for temperature is then made if needed. The measured reactivity values obtained for the fuel assembly, converter assembly and the H<sub>2</sub>O filled assembly were 2.41% $\Delta k/k$ , 2.24% $\Delta k/k$  and 2.88% $\Delta k/k$  respectively.

The procedure used to calculate the reactivity worth of a fuel assembly was to first make a computer run using twenty-four assemblies and then eliminate one assembly from

the proper geometric location, replacing it with moderator, re-running the program for the twenty-three assemblies. The difference in reactivity obtained from the two runs is the calculated reactivity worth of one assembly. The value obtained was  $(1.74 \pm .83)\% \Delta k/k$ .

For the case of the converter assembly, an additional box type had to be added describing the converter and then added to the array in its proper location. The KENO result of this measurement was  $(1.84 \pm 0.75)\% \Delta k/k$ .

The remaining measurement is the  $H_2O$  filled element. This is a fuel assembly modified by welding so that it could be filled with light water without fear of contaminating the heavy water. The reactivity worth of an  $H_2O$  filled element was calculated for two different cases by KENO. In the first case, the worth of an element filled with light water was represented by a lethargy weighted cross section and in the second case, the light water was represented by the fission spectrum weighted cross section. The results of these KENO runs are as follows: for the lethargy case the worth was  $(1.99 \pm 0.86)\% \Delta k/k$  and for the fission spectrum weighted case,  $(2.08 \pm 0.86)\% \Delta k/k$ .

## VI. SUMMARY AND CONCLUSIONS

The advantage of the three-dimensional aspect of the Monte Carlo method was decreased somewhat by the need to limit the input, thereby reducing the storage space required, and the need to find ways to reduce the running time. As was shown, this was accomplished by various methods such as homogenization of material, the use of albedo functions and the proper statistical weighting. Even with these disadvantages, the ability to describe portions of the reactor in a three-dimensional arrangement along with the fact that the core could be analyzed with the control rods included provide a significantly different approach to criticality calculations involving the ALRR.

Once the reactor was described in sufficient detail, it was found that a number of runs had to be made in order to verify the proper use of cross sections, albedos, etc. Once this had been done, it was then possible to make a series of runs to verify the accuracy of the program by comparing reactivity values obtained from the program to reactivity values obtained from reactor measurements. Table 8. summarizes the results of these runs. The first of these runs, the control rod worths and shutdown margin were found to give very good results.

Although the results were extremely close, a degree of caution should be exercised since the actual control rod

Table 8. Summary of KENO results and reactor measurements

Run	Reactor Measurement $\% \Delta k/k$	KENO Calculation $\% \Delta k/k$
control rod worth	27.69	27.84 $\pm$ 1.03
reactor shutdown margin	14.86	14.90 $\pm$ 0.78
thermal shield	1.48	1.99 $\pm$ 0.79
ALRR fuel assembly	2.41	1.74 $\pm$ 0.83
CP-5 converter assembly	2.24	1.84 $\pm$ 0.75
ALRR H <sub>2</sub> O filled assembly	2.88	--
501 cross-section	--	2.08 $\pm$ 0.86
502 cross-section	--	1.99 $\pm$ 0.86



measurements may deviate  $\pm 5\%$ .

It is well to note, even with the core modeled in a slightly super critical condition, the reactivity determined from the difference between runs gave fairly accurate answers. It was also observed from these data that the accuracy increased as the magnitude of the reactivity change increased. That is, the deviation of the control rod worths was about 5% of the total worth while the deviation of the fuel assembly worth was about 30% even though the fuel measurement was based upon a third more neutron histories. This correlates with what G. E. Whitesides has said in an article on the Monte Carlo method (14), in which he implies that for the calculation of a  $\Delta k$  between two cases to be meaningful, the  $\Delta k$  would have to be large with respect to the estimated standard deviation associated with the calculation.

The converter measurement represents the ability for the KENO program to handle reactivity worth measurements in locations other than a fuel assembly or control rod location. The converter was measured in the center experimental facility location, which is located in the center of the core. The reactivity worth of this converter, as calculated by KENO, was less than the measured value; but, again, the measured value fell within the limits of deviation with the statistics based upon a minimum of 22,240 neutron histories.

As shown in the case of the fuel assembly, the value of reactivity associated with the standard deviation is about a third of the mean value for k-effective. Even though there is a large deviation in the case of the smaller reactivity measurements, the consistency of the measured value being within the deviation allows the reactor physicist to include the deviation and predict whether or not an experiment will violate the operating limit concerning excess reactivity loading with a high reliability even though the exact value of the experiment can not be predicted to the same accuracy.

The reactivity calculation for the H<sub>2</sub>O filled assembly was the only case where the results of KENO did not span the measured reactivity value when the deviation was considered. This calculation was made for two cases. The first case used the fission spectrum weighted cross section for the light water and its result did include the measured value when the deviation was considered. The second case used the lethargy weighted cross section for light water. The results from that calculation were slightly less than the first case and when the deviation was included, the measured value was not spanned. Neither calculated value was in close agreement with the measured value and upon further investigation into the matter, it was found that other users of KENO (15) had found similar problems when trying to calculate cases where abrupt changes in cross section occurred in small quantities,

such as the small volume of  $H_2O$  in the  $D_2O$  moderated core. It was also indicated that the authors of KENO were working on a tracking system that would relieve the problem.

The difference obtained between the two cases of the light water element is significant since it shows the effect of the different cross sections, even though only a small fraction of the core was involved. The volume of moderator in one element is less than 2500 cubic centimeters which is very small compared to the  $D_2O$  inventory of approximately 2,600,000 cubic centimeters in the reflector region.

In a program such as KENO, there is always room for continual improvement. Up-dating cross section libraries, adding changes such as mentioned in the previous paragraph, modifying routines in order to decrease the amount of computer time; but in the mean time, KENO appears to be a useful tool at ALRR for predicting reactivity changes above  $2\% \Delta k/k$ .



## VII. BIBLIOGRAPHY

1. J. V. Uspensky, Introduction to Mathematical Probability, McGraw Hill, New York, 1937, p 203.
2. G. E. Whitesides and N. F. Cross, "KENO, A Multigroup Monte Carlo Criticality Program," CTC-5, Union Carbide Corporation, (1969).
3. M. H. Kalos and H. S. Wilf, Nucleonics, 15, No. 5, 64 (1957).
4. H. Rief and H. Kschwendt, Nucl. Sci. Eng., 30, No. 3, 395 (1967).
5. M. R. Mendelson, Nucl. Sci. Eng., 32, 319 (1968).
6. D. C. Irving, R. M. Freestone, Jr. and F. B. K. Kam, "O5R, A General-Purpose Monte Carlo Neutron Transport Code," ORNL-3622 (1965).
7. E. R. Woodcock, T. Murphy, P. J. Hemmings and T. C. Longworth, "Proceedings of the Conference on the Application of Computing Methods to Reactor Problems," ANL 7050, (May 1965) p 557.
8. P. J. Hemmings, "The GEM Code," AHSB (S) R 105 United Kingdom Atomic Energy Authority (1967).
9. J. C. Crudele, Ph.D. Thesis, Iowa State University, Ames, Iowa, 1973.
10. T. B. Fowler, M. L. Tobia and D. R. Vondy, "Exterminator-2, A Fortran-IV Code for Solving Multigroup Neutron Diffusion Equations in Two Dimensions," ORNL-4078 (1967).
11. AMF ATOMICS, "Final Hazards Summary Report for Ames Laboratory Research Reactor, Ames, Iowa," American Machine & Foundry Company, Greenwich, Conn., (1964).
12. G. E. Hansen and W. H. Roach, "Six and Sixteen Group Cross Sections for Fast and Intermediate Critical Assemblies," LAMS-2543 (1961).
13. E. C. Crume, Jr., "Proceedings of the Livermore Array Symposium," Conf- 680909, p 24 (1968).



14. G. E. Whitesides and K. D. Lathrop, "UC-46--Criticality Studies," ORNL-Y-CDC-11, (1972).
15. G. E. Whitesides, Union Carbide Corporation, (ORNL), Private communication, 1973.
16. H. Etherington, Nuclear Engineering Handbook, McGraw Hill, New York, 1958.

## VIII. ACKNOWLEDGEMENTS

The author wishes to express his sincere appreciation to Dr. Glenn Murphy, who displayed infinite patience with a part time student and gave 10 years of valuable guidance. Also, Dr. Glenn Murphy was very instrumental, not once but twice, in making it possible for the author to continue his education. Once at the undergraduate level and again at the graduate level for which the author is extremely grateful.

The author wishes to thank Dr. Richard Danofsky, whose leadership and guidance have made it possible for the author to achieve a long sought goal.

Finally the author wishes to dedicate this thesis to his wife Janet, who provided constant encouragement over the many years and whose efforts in the preparation of this thesis are greatly appreciated.

## IX. APPENDIX A: CROSS SECTIONS ON TAPE

## A. Available Albedos

## DIFFERENTIAL ALBEDO, 4 INCIDENT ANGLES

ID NUMBER	DESCRIPTION
1012	12 INCH WATER
2012	12 INCH PARAFIN
3080	78.74 INCH CARBON
4012	12 INCH POLYETHYLENE
5004	4 INCH CONCRETE
5008	8 INCH CONCRETE
5012	12 INCH CONCRETE
5016	16 INCH CONCRETE
5024	24 INCH CONCRETE

## ALBEDOS AND TRANSMISSIONS, 4 ANGLES

-5004	4 INCH CONCRETE
-5008	8 INCH CONCRETE
-5012	12 INCH CONCRETE
-5016	16 INCH CONCRETE

## B. Mixtures

<u>MIXTURE</u>	<u>DENSITY</u>	<u>NUMBER_DENSITY</u>	<u>ID_NUMBER</u>
Carbon Steel	7.82g/cc	C=.003921, Fe=.083491	00100
304 Stainless Steel	7.9g/cc	C=3.1691-4, Cr=1.6471-2 Mn=1.7321-3, Fe=6.036-2 Ni=6.4834-3, Si=1.694-3	00200
Oak Ridge Concrete	2.3g/cc	H=.0085 C=.0202 O=.0355, Ca=.0111 Si=.0017, Mg=.00186 Fe=1.93-4, Al=5.56-4 K=4.03-5, Na=1.63-5	00300
X(E) Polyethylene	0.92g/cc	H=.079433, C=.039716	00401
dE/E Polyethylene			00402
X(E) Water	.9982g/cc	H=.066743, O=.033372	00501
dE/E Water			00502
X(E) Plexiglas	1.182g/cc	H=.056884, C=.035552	00601
dE/E Plexiglas		O=.014221	00602



## C. Elements

<u>ID NUMBER</u>	<u>ELEMENT</u>
1101	HYDROGEN X (E)
1102	HYDROGEN DE/E
1201	DEUTERIUM X (E)
3100	LITHIUM-6
3200	LITHIUM-7
4100	BERYLLIUM
5100	BORON
6100	CARBON
7100	NITROGEN
8100	OXYGEN
9100	FLUORINE
11100	SODIUM
12100	MAGNESIUM
13100	ALUMINUM
14100	SILICON
16100	SULFUR
17100	CHLORINE
19100	POTASSIUM
20100	CALCIUM
22100	TITANIUM
23100	VANADIUM
24100	CHROMIUM
25100	MANGANESE
26100	IRON
27100	COBALT
28100	NICKEL
29100	COPPER
30100	ZINC
40100	ZIRCONIUM
41100	NIObIUM
42100	MOLYBDENUM
48100	CADMIUM
49100	INDIUM
58100	CERIUM
62100	SAMARIUM
63100	EUROPIUM
64100	GADOLINIUM
73100	TANTALUM
74100	TUNGSTEN
82100	LEAD
90104	TH-232 SIG P # 50
90108	TH-232 SIG P # 1000
90109	TH-232 SIG P # 1250
90110	TH-232 SIG P # 1500
90111	TH-232 SIG P # 1750

<u>ID NUMBER</u>	<u>ELEMENT</u>
90112	TH-232 SIG P # 2000
90113	TH-232 SIG P # 2500
90114	TH-232 SIG P # 3000
90115	TH-232 SIG P # 3500
92300	U-233
92301	U-233-1 SIG P # 20
92302	U-233-2 SIG P # 40
92303	U-233-3 SIG P # 60
92304	U-233-4 SIG P # 100
92305	U-233-5 SIG P # 200
92306	U-233-6 SIG P # 400
92307	U-233-7 SIG P # 600
92308	U-233-8 SIG P # 1000
92309	U-233-9 SIG P # 2000
92310	U-233-10 SIG P # 4000
92311	U-233-11 SIG P # 6000
92312	U-233-12 SIG P # 10000
92400	U-234
92500	U-235 YR
92501	U-235-1R SIG P # 20
92502	U-235-2R SIG P # 40
92503	U-235-3R SIG P # 60
92504	U-235-4R SIG P # 100
92505	U-235-5R SIG P # 200
92506	U-235-6R SIG P # 400
92507	U-235-7R SIG P # 600
92508	U-235-8R SIG P # 1000
92509	U-235-9R SIG P # 2000
92510	U-235-10R SIG P # 4000
92511	U-235-11R SIG P # 6000
92511	U-235-12R SIG P # 10000
92600	U-236
92800	U-238-Y
92801	U-238 SIG P # 12
92802	U-238 SIG P # 15
92803	U-238 SIG P # 20
92804	U-238 SIG P # 25
92805	U-238 SIG P # 30
92806	U-238 SIG P # 35
92807	U-238 SIG P # 40
92808	U-238 SIG P # 45
92809	U-238 SIG P # 50
92810	U-238 SIG P # 55
92811	U-238 SIG P # 60
92812	U-238 SIG P # 65
92813	U-238 SIG P # 70
92814	U-238 SIG P # 75
92815	U-238 SIG P # 80

<u>ID_NUMBER</u>	<u>ELEMENT</u>
92816	U-238 SIG P # 85
92817	U-238 SIG P # 90
92818	U-238 SIG P # 95
92819	U-238 SIG P # 100
92820	U-238 SIG P # 110
92821	U-238 SIG P # 120
92822	U-238 SIG P # 130
92823	U-238 SIG P # 140
92824	U-238 SIG P # 160
92825	U-238 SIG P # 180
92826	U-238 SIG P # 200
92827	U-238 SIG P # 220
92828	U-238 SIG P # 240
92829	U-238 SIG P # 260
92830	U-238 SIG P # 280
92831	U-238 SIG P # 300
92832	U-238 SIG P # 330
92833	U-238 SIG P # 360
92834	U-238 SIG P # 400
92835	U-238 SIG P # 450
92836	U-238 SIG P # 500
92837	U-238 SIG P # 550
92838	U-238 SIG P # 600
92839	U-238 SIG P # 650
92840	U-238 SIG P # 700
92841	U-238 SIG P # 800
92842	U-238 SIG P # 900
92843	U-238 SIG P # 1000
92844	U-238 SIG P # 1500
92845	U-238 SIG P # 2000
92846	U-238 SIG P # 3000
92847	U-238 SIG P # 4000
92848	U-238 SIG P # 5000
92849	U-238 SIG P # 6000
92850	U-238 SIG P # 8000
92851	U-238 SIG P # 10000
92852	U-238 SIG P # 20000
92853	U-238 SIG P # 40000
92854	U-238 SIG P # 60000
92855	U-238 SIG P # 100000
92856	U-238-1R SIG P # 20
92857	U-238-2R SIG P # 40
92858	U-238-3R SIG P # 60
92859	U-238-4R SIG P # 100
92860	U-238-5R SIG P # 200
92861	U-238-6R SIG P # 400
92862	U-238-7R SIG P # 600
94000	PU-240

<u>ID_NUMBER</u>	<u>ELEMENT</u>
94001	PU-240-1 SIG P # 50
94002	PU-240-2 SIG P # 100
94003	PU-240-3 SIG P # 200
94004	PU-240-4 SIG P # 400
94005	PU-240-5 SIG P # 600
94006	PU-240-6 SIG P # 1000
94007	PU-240-7 SIG P # 2000
94008	PU-240-8 SIG P # 4000
94009	PU-240-9 SIG P # 6000
94010	PU-240-10 SIG P # 10000
94011	PU-240-11 SIG P # 20000
94012	PU-240-12 SIG P # 40000
94013	PU-240-13 SIG P # 60000
94014	PU-240-14 SIG P # 100000
94015	PU-240-15 SIG P # 200000
94016	PU-240-16 SIG P # 400000
94017	PU-240-17 SIG P # 600000
94018	PU-240-18 SIG P # 1000000
94100	PU-241
94200	PU-242
94800	PU-238
94801	PU-238-1 SIG P # 100
94802	PU-238-2 SIG P # 1000
94803	PU-238-3 SIG P # 10000
98804	PU-238 Y
94900	PU-239
94901	PU-239-1 SIG P # 20
94902	PU-239-2 SIG P # 40
94903	PU-239-3 SIG P # 60
94904	PU-239-4 SIG P # 100
94905	PU-239-5 SIG P # 200
94906	PU-239-6 SIG P # 400
94907	PU-239-7 SIG P # 600
94908	PU-239-8 SIG P # 1000
94909	PU-239-9 SIG P # 2000
94910	PU-239-10 SIG P # 4000
94911	PU-239-11 SIG P # 6000
94912	PU-239-12 SIG P # 10000
94913	PU-239-13 SIG P # 20000
94914	PU-239-14 SIG P # 40000
94915	PU-239-15 SIG P # 60000
94916	PU-239-16 SIG P # 100000



## X. APPENDIX B: CALCULATION OF THE POTENTIAL

## SCATTERING CROSS SECTION OF THE FUEL MIXTURE

In order to select the proper cross section for U235 and U238 from the list supplied in the previous section,  $\sigma_p$  (SIG P) for the fuel must be calculated. SIG P is calculated as follows:

$$\text{SIG P} = \sum \sigma_{si} N_i / N_f$$

$\sigma_{si}$  is the scattering cross section at the applicable energy for each nuclide

$N_i$  is the nuclei density for each nuclide

$N_f$  is the nuclei density for the fuel in question

For the ALRR fuel assembly, the fuel is composed of U238, U235 and aluminum. The nuclei densities being 3.459 E-05, 4.755 E-04 and 5.9607 E-02 respectively. The thermal scattering cross-sections (16) are U235 (10b), U238 (8.3b) and Al (1.4b), where b = barns. The resulting SIG P for U235 is 186b and for U238 it was 2558b. Knowing SIG P, one can then select the proper nuclide from the table.

## XI. APPENDIX C: CALCULATION OF REACTIVITY WORTH AND DEVIATION

This calculation consists of converting a value of k-effective and its corresponding deviation into a  $\% \Delta k/k$  value with its deviation and then, in some cases, finding the difference between two reactivity worths in  $\% \Delta k/k$  and its corresponding deviation. The relationship between  $\Delta k/k$  and k-effective is as usual:  $\Delta k/k = (k\text{-eff} - 1.0)/k\text{-eff}$ . To find the deviation, it is necessary to first consider the numerator alone which is in the form of  $y \pm x$  where the deviation is  $p_{\text{num}} = \pm \sqrt{(p_x^2 + p_y^2)}$ .

Since the deviation of the critical condition (1.0) is zero, then obviously the deviation of the numerator is just the deviation of k-effective. The form of the equation then becomes  $x/y$  where  $p = \pm \sqrt{(y^2 p_x^2 + x^2 p_y^2)}/y^2$  but from above  $p_x = p_y$  so  $p = \pm p_x \sqrt{(y^2 + x^2)}/y^2$  where  $y = k\text{-eff}$  and  $x = k\text{eff}-1$  and  $p_x$  is the standard deviation of k-effective. At this point, k-effective can be converted to a  $\Delta k/k$  value along with its deviation. If two values of  $\Delta k/k$  are subtracted, then the first form ( $x \pm y$ ) applies and the new deviation can be calculated.